Superfluidity of dipole excitons in the presence of band gaps in two-layer graphene

Oleg L. Berman,[1,2] Roman Ya. Kezerashvili,[1,2] and Klaus Ziegler[3]

[1]*Physics Department, New York City College of Technology, The City University of New York, Brooklyn, New York 11201, USA*

[2]*The Graduate School and University Center, The City University of New York, New York, New York 10016, USA*

[3]*Institut für Physik, Universität Augsburg, D-86135 Augsburg, Germany*

(Received 17 November 2011; revised manuscript received 16 December 2011; published 13 January 2012)

We propose to observe superfluidity of quasi-two-dimensional dipole excitons in double-layer graphene in the presence of band gaps. The energy spectrum of the collective excitations, the sound spectrum, and the effective exciton mass are functions of the energy gaps, density, and interlayer separation. The superfluid density n_s and temperature of the Kosterlitz-Thouless phase transition T_c are decreasing functions of the energy gaps.

DOI: 10.1103/PhysRevB.85.035418 PACS number(s): 71.35.Lk, 78.67.Wj

I. INTRODUCTION

Many-particle systems of spatially indirect dipole excitons in coupled quantum wells (CQW's) have been the subject of recent experimental investigations.[1–3] These systems are of interest, in particular, in connection with the possibility of superfluidity of dipole excitons or electron-hole pairs.[4–7] Graphene has been attracting a great deal of experimental and theoretical attention because of unusual properties in its band structure. Due to the absence of a gap between the conduction and valence bands in graphene, the screening effects result in the absence of excitons in graphene. However, a gap in the electron spectrum in graphene can be opened by applying the magnetic field, which results in the formation of magnetoexcitons,[8] and the effective mass of magnetoexciton increases when magnetic field increases, and, therefore, the Kosterlitz-Thouless critical temperature of the superfluidity decreases with an increasing magnetic field. BEC and superfluidity of spatially indirect magnetoexcitons with spatially separated electrons and holes in high magnetic field have been studied in graphene double layers[9] and graphene superlattices.[10,11] The electron-hole pair condensation in the graphene-based bilayers has been studied in Refs. 12–15.

In this paper, we propose a physical realization of an excitonic superfluidity in two parallel graphene layers, when one layer is filled by electrons and the other is filled by holes. We consider the formation of excitons in two parallel graphene layers separated by an insulating material (e.g., SiO_2) due to gap opening in the electron and hole spectra in the two graphene layers. The advantage of considering an exciton formed by an electron and a hole in two different graphene layers, separated by an insulating slab, is that the dielectric slab creates a barrier for the electron-hole recombination that increases the lifetime of the exciton compared to the exciton formed by an electron and a hole in a single graphene layer. It was shown in Ref. 16 that a tunable gap in graphene can be induced and controlled by hydrogenation. The equilibrium system of local pairs of spatially separated electrons and holes can be created by a bias voltage between two graphene layers or between two gates located near the corresponding graphene layers (for simplicity, we also refer to these equilibrium local electron-hole pairs as indirect excitons). Excitons with spatially separated electrons and holes can be created also by laser pumping (far infrared in graphene) and by applying a perpendicular electric field as for CQW's.[1–3] We assume that the system is in a quasiequilibrium state and in the low-density regime for excitons, i.e., the exciton radius is restricted by $a < n^{-1/2}$, where n is the two-dimensional (2D) exciton density. In such a system, the effective exciton mass can be controlled by the gap. The effective exciton mass can be small relative to the mass of a free electron, and the Kosterlitz-Thouless transition temperature T_c can be controlled by the gaps.

The paper is organized in the following way. In Sec. II, we present the Hamiltonian of an electron and a hole in two different parallel graphene sheets, separated by a dielectric in the presence of the band gap. We obtain the single-particle energy spectrum of the dipole exciton in two-layer graphene and find its effective mass. In Sec. III, we study the condensation of a gas of excitons and calculate the density of the superfluid component as well as the Kosterlitz-Thouless temperature. Finally, a discussion of the results and the conclusions follow in Sec. IV.

II. SINGLE DIPOLE EXCITON

We consider an electron and a hole located in two different graphene sheets. Obviously the gaps in these sheets are independent, and in the general case we can introduce two nonequal gaps δ_1 and δ_2, corresponding to the first and second graphene sheet, respectively. We assume that our exciton is formed by the electron located in one graphene sheet and, correspondingly, the hole located in the other. The gap parameters δ_1, δ_2 are a consequence of adatoms on the graphene sheets (e.g., by hydrogen, oxygen, or other noncarbon atoms[17]), which create a one-particle potential.

Since the motion of the electron is restricted in one graphene sheet and the motion of the hole is restricted in the other graphene sheet, we replace the coordinate vectors of the electron and the hole by their projections $\mathbf{r}_1$ and $\mathbf{r}_2$ on the plane of one of the graphene sheets. These new in-plane coordinates $\mathbf{r}_1$ and $\mathbf{r}_2$ will be used hereafter in our paper. Thus, we reduce the restricted 3D two-body problem to a 2D two-body problem. Each honeycomb lattice is characterized by the coordinates $(\mathbf{r}_j,1)$ on sublattice A and $(\mathbf{r}_j,2)$ on sublattice B. Then the two-particle wave function, describing two particles in different sheets, reads $\Psi(\mathbf{r}_1,s_1;\mathbf{r}_2,s_2)$. This wave function can also be understood as a four-component spinor, where the spinor components refer to the four possible values of the

sublattice indices s_1, s_2,

$$\Psi(\mathbf{r}_1, s_1; \mathbf{r}_2, s_2) = \begin{pmatrix} \phi_{aa}(\mathbf{r}_1, \mathbf{r}_2) \\ \phi_{ab}(\mathbf{r}_1, \mathbf{r}_2) \\ \phi_{ba}(\mathbf{r}_1, \mathbf{r}_2) \\ \phi_{bb}(\mathbf{r}_1, \mathbf{r}_2) \end{pmatrix} . \tag{1}$$

The system of two interacting particles located in different graphene sheets with a broken sublattice symmetry in each can be described by the Hamiltonian

$$\mathcal{H} = \begin{pmatrix} -\delta_1 + \delta_2 + V & d_2 & d_1 & 0 \\ d_2^\dagger & -\delta_1 - \delta_2 + V & 0 & d_1 \\ d_1^\dagger & 0 & \delta_1 + \delta_2 + V & d_2 \\ 0 & d_1^\dagger & d_2^\dagger & \delta_1 - \delta_2 + V \end{pmatrix} , \tag{2}$$

where $V(r) = -\frac{e^2}{\varepsilon\sqrt{r^2+D^2}}$ is the electron-hole attraction, e is the electron charge, ε is the dielectric constant of the dielectric between graphene sheets, D is the interlayer separation, $\mathbf{r}$ is the difference between the positions of an electron and a hole on the plane parallel to the graphene sheets, $d_j = \hbar v_F(-i\frac{\partial}{\partial x_j} - \frac{\partial}{\partial y_j})$, and $d_j^\dagger = \hbar v_F(-i\frac{\partial}{\partial x_j} + \frac{\partial}{\partial y_j})$, $j = 1,2$; x and y are components of the vectors $\mathbf{r}_1$ and $\mathbf{r}_2$ that represent the coordinates of the electron and hole, respectively, and $v_F = \sqrt{3}at/(2\hbar)$ is the Fermi velocity of electrons in graphene, where $a = 2.566$ Å is a lattice constant and $t \approx 2.71$ eV is the overlap integral between the nearest carbon atoms.[18]

In Hamiltonian (2), the center-of-mass energy cannot be separated from the relative motion even though the interaction $V = V(r)$ depends only on the the relative motion. This is caused by the chiral nature of the Dirac electron in graphene. A similar conclusion was made for the two-particle problem in graphene in Ref. 19. Let us mention that at $\delta_1 = \delta_2 = 0$ and $D = 0$, the Hamiltonian (2) is identical to the Hamiltonian (2) in Ref. 19 representing the two-particle problem in one graphene sheet if the band gap is absent.

Since the electron-hole Coulomb interaction depends only on the relative coordinate, we introduce the new "center-of-mass" coordinates in the plane of a graphene sheet (x,y):

$$\mathbf{R} = \alpha\mathbf{r}_1 + \beta\mathbf{r}_2 , \qquad \mathbf{r} = \mathbf{r}_1 - \mathbf{r}_2 . \tag{3}$$

The coefficients α and β will be found below from the condition of the separation of the coordinates of the center-of-mass and relative motion in the Hamiltonian in the one-dimensional "scalar" equation determining the corresponding component of the wave function.

We are looking for the wave function in the form

$$\Psi_j(\mathbf{R}, \mathbf{r}) = \mathrm{e}^{i\mathcal{K}\cdot\mathbf{R}}\, \psi_j(\mathbf{r}) . \tag{4}$$

Using the following notations:

$$\begin{gathered} \mathcal{K}_+ = \mathcal{K}\mathrm{e}^{i\Theta} = \mathcal{K}_x + i\mathcal{K}_y , \quad \mathcal{K}_- = \mathcal{K}\mathrm{e}^{-i\Theta} = \mathcal{K}_x - i\mathcal{K}_y , \\ \Theta = \tan^{-1}\left(\frac{\mathcal{K}_y}{\mathcal{K}_x}\right) , \end{gathered} \tag{5}$$

we can rewrite (2) in terms of the representation of the coordinates $\mathbf{R}$ and $\mathbf{r}$ in the final form as

$$\mathcal{H} = \left(\begin{array}{cc|cc} V(r) - \delta_1 + \delta_2 & \hbar v_F(\beta\mathcal{K}_- + i\partial_x + \partial_y) & \hbar v_F(\alpha\mathcal{K}_- - i\partial_x - \partial_y) & 0 \\ \hbar v_F(\beta\mathcal{K}_+ + i\partial_x - \partial_y) & V(r) - \delta_1 - \delta_2 & 0 & \hbar v_F(\alpha\mathcal{K}_- - i\partial_x - \partial_y) \\ \hline \hbar v_F(\alpha\mathcal{K}_+ - i\partial_x + \partial_y) & 0 & V(r) + \delta_1 + \delta_2 & \hbar v_F(\beta\mathcal{K}_- + i\partial_x + \partial_y) \\ 0 & \hbar v_F(\alpha\mathcal{K}_+ - i\partial_x + \partial_y) & \hbar v_F(\beta\mathcal{K}_+ + i\partial_x - \partial_y) & V(r) + \delta_1 - \delta_2 \end{array}\right) , \tag{6}$$

where $\partial_x = \partial/\partial x$, $\partial_y = \partial/\partial y$, and x and y are the components of $\mathbf{r}$.

The eigenvalue equation for the two-particle problem can be represented in the following form:

$$\mathcal{H}\Psi = \epsilon\Psi, \quad \Psi = \begin{pmatrix} \Psi_a \\ \Psi_b \end{pmatrix}, \quad \text{where} \quad \Psi_a = \begin{pmatrix} \phi_{aa} \\ \phi_{ab} \end{pmatrix}, \quad \Psi_b = \begin{pmatrix} \phi_{bb} \\ \phi_{ba} \end{pmatrix} . \tag{7}$$

The two components mean that one particle is on sublattice $a(b)$ and the other particle is on sublattice $a(b)$, respectively. This eigenvalue equation is a first-order differential equation for a four-component spinor. It is possible to rewrite this equation in terms of two second-order differential equations for the two-component spinors ψ_a and ψ_b. Assuming that the interaction potential and

both relative and center-of-mass kinetic energies are small compared to the gaps δ_1 and δ_2, we obtain for the eigenvalue problem of the spinor component ϕ_{aa} the equation (see Appendix)

$$\left(-\delta_1+\delta_2+V(r)+\hbar^2v_F^2\frac{\alpha^2\mathcal{K}^2-\nabla_r^2-2i\alpha(\mathcal{K}_x\partial_x+\mathcal{K}_y\partial_y)}{\epsilon-\delta_1-\delta_2}+\hbar^2v_F^2\frac{\beta^2\mathcal{K}^2-\nabla_r^2+2i\beta(\mathcal{K}_x\partial_x+\mathcal{K}_y\partial_y)}{\epsilon+\delta_1+\delta_2}\right)\phi_{aa}=\epsilon\phi_{aa}\ . \tag{8}$$

Choosing the values for the coefficients α and β to separate the coordinates of the center-of-mass and relative motion in Eq. (8), we have

$$\alpha=\frac{\epsilon-(\delta_1+\delta_2)}{2\epsilon},\qquad \beta=\frac{\epsilon+(\delta_1+\delta_2)}{2\epsilon}\ . \tag{9}$$

Substituting Eq. (9) into Eq. (8), assuming $r\ll D$, and, therefore, using the Taylor expansion for the interaction potential up to the second-order term $V(r)=-V_0+\gamma r^2$ in Eq. (8), we obtain

$$\left(-\frac{\epsilon(\hbar v_F)^2\nabla_r^2}{2[\epsilon^2-(\delta_1+\delta_2)^2]}+\gamma r^2\right)\phi_{aa}=\left[\epsilon+\delta_1-\delta_2+V_0-\frac{(\hbar v_F\mathcal{K})^2}{2\epsilon}\right]\phi_{aa}\ , \tag{10}$$

where $V_0=e^2/(\varepsilon D)$ and $\gamma=e^2/(2\varepsilon D^3)$. Equation (10) can be rewritten in the form of the two-dimensional isotropic harmonic oscillator:

$$\left[-\mathcal{F}_1(\epsilon)\nabla_r^2+\gamma r^2\right]\phi_{aa}=\mathcal{F}_0(\epsilon)\phi_{aa}\ , \tag{11}$$

where

$$\mathcal{F}_1=\frac{\epsilon(\hbar v_F)^2}{2[\epsilon^2-(\delta_1+\delta_2)^2]}\ ,\qquad \mathcal{F}_0=\epsilon+V_0+\delta_1-\delta_2-\frac{(\hbar v_F\mathcal{K})^2}{2\epsilon}\ . \tag{12}$$

The solution of the harmonic oscillator equation (11) is well known and is given by

$$\frac{\mathcal{F}_0(\epsilon)}{\mathcal{F}_1(\epsilon)}=2N\sqrt{\frac{\gamma}{\mathcal{F}_1(\epsilon)}}\ , \tag{13}$$

where $N=2n_1+n_2+1$; $n_1=0,1,2,3,\ldots$ and $n_2=0,\pm1,\pm2,\pm3,\ldots,\pm n_1$ are the quantum numbers.

The expansion of Eq. (13) up to second order in $\mathcal{K}$ (i.e., for $\hbar v_F\mathcal{K}\ll\delta_1+\delta_2$) gives for the energy

$$\epsilon=-V_0+\mu\sqrt{1+\frac{C_1}{\mu^3}}+\frac{\mathcal{K}^2}{2M}\ , \tag{14}$$

where we have introduced the parameters $\mu=\delta_1+\delta_2$ and $C_1=2\gamma N^2(\hbar v_F)^2$. When we further assume that $C_1\ll\epsilon(\epsilon^2-\mu^2)$ and $\delta_1\approx\delta_2$, the effective exciton mass M reads

$$M=\frac{\mu^4}{v_F^2C_1}\sqrt{1+\frac{C_1}{\mu^3}}\ . \tag{15}$$

The effective exciton mass M as a function of total energy gap $\delta_1+\delta_2$ and the different interlayer separation D defined by Eq. (15) is plotted in Fig. 1(a). According to Fig. 1(a), the effective exciton mass M increases when the total energy gap increases and the interlayer separation D increases. Let us mention that for the excitons in CQW's, the effective exciton mass does not depend on the interlayer separation, because the electrons and holes in CQW's are described by a Schrödinger Hamiltonian, while excitons in two graphene layers are described by the Dirac-like Hamiltonian (6).

Due to the interlayer separation D, indirect excitons both in a ground state ($n_1=n_2=0$) and in excited states have nonzero electric dipole moments. We suppose that indirect excitons interact as *parallel* dipoles. This is valid when $D\ll\langle r\rangle$, where r is the length of the vector between the positions of an electron and a hole, projected onto the plane parallel to graphene sheets.

III. SUPERFLUIDITY OF THE EXCITONIC GAS

At zero temperature $T=0$, the dilute gas of excitons, which is a boson system, forms a Bose-Einstein condensate.[20] Therefore, the system of indirect excitons can be treated by the diagram technique for a boson system. For the dilute 2D exciton system (at $na^2\ll1$), the summation of ladder diagrams can be used, since we treat the exciton system as the weakly interacting Bose system. The integral equation for vertex Γ in the ladder approximation is represented in Ref. 21. In the ladder approximation, the chemical potential $\mu_{\rm ex}$ is

$$\mu_{\rm ex}=\frac{\pi\hbar^2n}{sM\ln[s\hbar^4\varepsilon^2/(2\pi nM^2e^4D^4)]}\ , \tag{16}$$

where $s=4$ is the spin degeneracy factor. The collective excitations are characterized by the sound spectrum $\epsilon(P)=c_sP$ with the sound velocity $c_s=\sqrt{\mu_{\rm ex}/M}$. Thus, the collective excitations spectrum depends on the energy gaps, the interlayer separation, and the exciton density. Since excitons have a sound spectrum of collective excitations at small momenta due to the dipole-dipole repulsion, the excitonic superfluidity is possible at small temperatures T in double-layer graphene because the sound spectrum satisfies the Landau criterion of superfluidity.

The dilute excitons constructed by spatially separated electrons and holes in double-layer graphene at large interlayer separations when $V_0\ll\delta_1$ and $V_0\ll\delta_2$ form a 2D weakly interacting gas of bosons with the pair dipole-dipole repulsion. So the superfluid-normal phase transition in this system is the Kosterlitz-Thouless transition,[22] and the temperature of

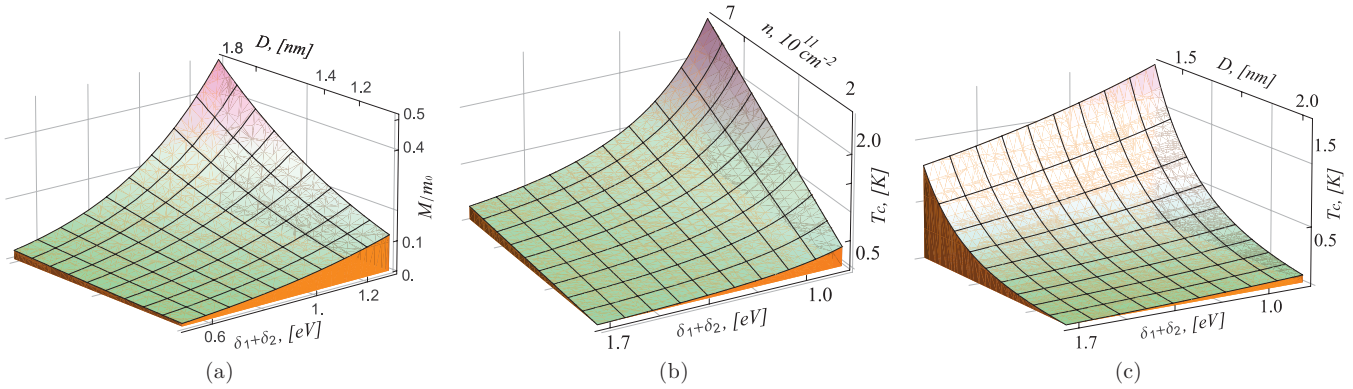

FIG. 1. (Color online) The dependence of the effective exciton mass on the total energy gap and graphene interlayer separations (a). The dependence of the Kosterlitz-Thouless transition temperature T_c on the total energy gap and the exciton concentration (b) and on the total energy gap and and the graphene interlayer separations (c).

this transition T_c in a two-dimensional exciton system is determined by the equation

$$T_c = \frac{\pi\hbar^2 n_s(T_c)}{2k_B M}, \tag{17}$$

where $n_s(T)$ is the superfluid density of the exciton system as a function of temperature T, and k_B is Boltzmann's constant. We obtain the superfluid density as $n_s = n - n_n$ by determining the density of the normal component n_n when we follow the procedure[20] as a linear response of the total momentum with respect to the external velocity:

$$n_s = n - \frac{3\zeta(3)}{2\pi\hbar^2}\frac{k_B^3 T^3}{c_s^4 M}. \tag{18}$$

It turns out that the expression for the superfluid density n_s in the two-layer graphene in the presence of the band gaps for the dilute exciton system differs from the analogous expression in semiconductor CQW's [compare with Ref. 7 by replacing the total exciton mass $M = m_e + m_h$ with the effective exciton mass M given by Eq. (15)].

In a 2D system, superfluidity of excitons appears below the Kosterlitz-Thouless transition temperature.[22] Using Eq. (18), we obtain an equation for the Kosterlitz-Thouless transition temperature T_c. The Kosterlitz-Thouless transition temperature T_c as a function of the total energy gap $\delta_1 + \delta_2$ and the exciton concentration n at the fixed interlayer separation $D = 1.2$ nm is presented in Fig. 1(b). The Kosterlitz-Thouless transition temperature T_c as a function of the total energy gap $\delta_1 + \delta_2$ and the interlayer separation D at the fixed exciton concentration $n = 5 \times 10^{11}$ cm^{-2} is presented in Fig. 1(c). It can be seen that T_c decreases when both the interlayer separation D and the total energy gap $\delta_1 + \delta_2$ are increasing.

IV. DISCUSSION

The advantage of observing the exciton superfluidity and BEC in graphene in comparison with those in CQW's is based on the fact that the exciton superfluidity and BEC in graphene can be controlled by the gaps that depend on doping. Note that we considered the superfluidity in two cases: first, an equilibrium system of electrons and holes created by the gates, and second, the electrons and holes created by the laser pumping such that the excitons are in a quasiequilibrium thermodynamic state.

The lifetime of indirect excitons in double-layer graphene is restricted by the electron-hole recombination. The latter is due to electron-hole tunneling through the dielectric barrier between the graphene layers, which depends on the dielectric constant of the material and its thickness D. This is similar to the case of indirect excitons in the coupled quantum wells, which are separated by a dielectric barrier. For instance, in GaAs/AlGaAs coupled quantum wells, the experimentally observed lifetime of an indirect exciton is around 100 ns for the dielectric barrier $D = 4.2$ nm (Ref. 23) and around 50 ns for $D = 11.5$ nm.[24] Another possible effect on the lifetime of excitons is the formation of more complex excitations, such as trions. In the latter, the constituting particles have to overcome a Coulomb barrier. Therefore, their lifetime is rather short in comparison with the excitons.

In conclusion, we propose a physical realization to observe superfluidity of quasi-two-dimensional dipole excitons in two-layer graphene in the presence of band gaps. The effective exciton mass is calculated as a function of the electron and hole energy gaps in the graphene layers, density, and interlayer separation. We demonstrate the rise of the effective exciton mass with the increase of the gaps and interlayer separation. The dependence of the exciton mass on the electron-hole Coulomb attraction and interlayer distance comes from the Dirac-like spectrum of electrons and holes. We show that the superfluid density n_s and the Kosterlitz-Thouless temperature T_c increase with the rise of the excitonic density n and decrease with the rise of the gaps δ_1 and δ_2 as well as the interlayer separation D, and therefore they could be controlled by these parameters.

ACKNOWLEDGMENTS

The authors acknowledge support from the Center for Theoretical Physics of the New York City College of Technology, CUNY and from the Deutsche Forschungsgemeinschaft through Grant No. ZI 305/5-1.

APPENDIX: EIGENVALUE PROBLEM FOR TWO PARTICLES

Using the definitions

$$\mathcal{O}_1 = \hbar v_F \begin{pmatrix} \alpha\mathcal{K}_- - i\partial_x - \partial_y & 0 \\ 0 & \alpha\mathcal{K}_- - i\partial_x - \partial_y \end{pmatrix}, \quad \text{(A1)}$$

$$\mathcal{O}_2 = \hbar v_F \begin{pmatrix} 0 & \beta\mathcal{K}_- + i\partial_x + \partial_y \\ \beta\mathcal{K}_+ + i\partial_x - \partial_y & 0 \end{pmatrix}, \quad \text{(A2)}$$

the eigenvalue problem $\mathcal{H}\Psi = \epsilon\Psi$ results in the following equations:

$$\begin{aligned} &[\mathcal{O}_2 + V(r)\sigma_0 - \delta_1\sigma_0 + \delta_2\sigma_3]\,\Psi_a + \mathcal{O}_1\Psi_b = \epsilon\sigma_0\Psi_a, \\ &\mathcal{O}_1^\dagger\Psi_a + [\mathcal{O}_2 + V(r)\sigma_0 + \delta_1\sigma_0 + \delta_2\sigma_3]\,\Psi_b = \epsilon\sigma_0\Psi_b\,. \end{aligned} \quad \text{(A3)}$$

The second equation gives us

$$\Psi_b = [\epsilon\sigma_0 - \mathcal{O}_2 - V(r)\sigma_0 - \delta_1\sigma_0 - \delta_2\sigma_3]^{-1}\,\mathcal{O}_1^\dagger\Psi_a\,. \quad \text{(A4)}$$

This can be inserted into the first equation of (A3) to get an equation for Ψ_a alone:

$$[\mathcal{O}_2 + V(r)\sigma_0 - \delta_1\sigma_0 + \delta_2\sigma_3]\,\Psi_a + \hbar^2 v_F^2 \frac{\left[\alpha^2\mathcal{K}^2 - \nabla_{\mathbf{r}}^2 - 2i\alpha(\mathcal{K}_x\partial_x + \mathcal{K}_y\partial_y)\right]}{\epsilon\sigma_0 - \delta_1\sigma_0 - \delta_2\sigma_3}\Psi_a = \epsilon\sigma_0\Psi_a\,. \quad \text{(A5)}$$

Here we have assumed that the interaction potential and both relative and center-of-mass kinetic energies are small compared to the gaps δ_1 and δ_2. This leads to

$$[\epsilon\sigma_0 - \mathcal{O}_2 - V(r)\sigma_0 - \delta_1\sigma_0 - \delta_2\sigma_3]^{-1} \simeq \frac{1}{\epsilon\sigma_0 - \delta_1\sigma_0 - \delta_2\sigma_3}\,. \quad \text{(A6)}$$

Now we rewrite Eq. (A5) for the individual spinor components as

$$\left(-\delta_1 + \delta_2 + V(r) + \hbar^2 v_F^2 \frac{\alpha^2\mathcal{K}^2 - \nabla_{\mathbf{r}}^2 - 2i\hbar v_F\alpha(\mathcal{K}_x\partial_x + \mathcal{K}_y\partial_y)}{\epsilon - \delta_1 - \delta_2}\right)\phi_{aa} + \hbar v_F\left(\beta\mathcal{K}_- + i\partial_x + \partial_y\right)\phi_{ab} = \epsilon\phi_{aa}\,, \quad \text{(A7)}$$

$$\hbar v_F\left(\beta\mathcal{K}_+ + i\partial_x - \partial_y\right)\phi_{aa} + \left(-\delta_1 - \delta_2 + V(r) + \hbar^2 v_F^2 \frac{\alpha^2\mathcal{K}^2 - \nabla_{\mathbf{r}}^2 - 2i\alpha(\mathcal{K}_x\partial_x + \mathcal{K}_y\partial_y)}{\epsilon - \delta_1 + \delta_2}\right)\phi_{ab} = \epsilon\phi_{ab} \quad \text{(A8)}$$

and obtain from the second equation

$$\phi_{ab} = \left[\epsilon + \delta_1 + \delta_2 - V(r) - \hbar^2 v_F^2 \frac{\alpha^2\mathcal{K}^2 - \nabla_{\mathbf{r}}^2 - 2i\alpha(\mathcal{K}_x\partial_x + \mathcal{K}_y\partial_y)}{\epsilon - \delta_1 + \delta_2}\right]^{-1}\left(\beta\mathcal{K}_+ + i\partial_x - \partial_y\right)\hbar v_F\phi_{aa}\,. \quad \text{(A9)}$$

Substituting ϕ_{ab} into Eq. (A7) gives us

$$\begin{aligned} &\left(-\delta_1 + \delta_2 + V(r) + \hbar^2 v_F^2 \frac{\alpha^2\mathcal{K}^2 - \nabla_{\mathbf{r}}^2 - 2i\alpha(\mathcal{K}_x\partial_x + \mathcal{K}_y\partial_y)}{\epsilon - \delta_1 - \delta_2}\right)\phi_{aa} + \hbar^2 v_F^2\left(\beta\mathcal{K}_- + i\partial_x + \partial_y\right) \\ &\quad\times\left[\epsilon + \delta_1 + \delta_2 - V(r) - \hbar^2 v_F^2 \frac{\alpha^2\mathcal{K}^2 - \nabla_{\mathbf{r}}^2 - 2i\alpha(\mathcal{K}_x\partial_x + \mathcal{K}_y\partial_y)}{\epsilon - \delta_1 + \delta_2}\right]^{-1}\left(\beta\mathcal{K}_+ + i\partial_x - \partial_y\right)\hbar v_F\phi_{aa} = \epsilon\phi_{aa}\,. \end{aligned} \quad \text{(A10)}$$

Assuming again that the interaction potential and both relative and center-of-mass kinetic energies are small compared to the gaps δ_1 and δ_2, we get from Eq. (A10) the following approximation:

$$\left[\epsilon + \delta_1 + \delta_2 - V(r) - \hbar^2 v_F^2 \frac{\alpha^2\mathcal{K}^2 - \nabla_{\mathbf{r}}^2 - 2i\alpha(\mathcal{K}_x\partial_x + \mathcal{K}_y\partial_y)}{\epsilon - \delta_1 + \delta_2}\right]^{-1} = \frac{1}{\epsilon + \delta_1 + \delta_2}\,, \quad \text{(A11)}$$

which gives for Eq. (A10) the scalar Eq. (8).

[1] D. W. Snoke, Science **298**, 1368 (2002).
[2] L. V. Butov, J. Phys. Condens. Matter **16**, R1577 (2004).
[3] J. P. Eisenstein and A. H. MacDonald, Nature (London) **432**, 691 (2004).
[4] Yu. E. Lozovik and V. I. Yudson, Sov. Phys. JETP **44**, 389 (1976).
[5] X. Zhu, P. B. Littlewood, M. S. Hybertsen, and T. M. Rice, Phys. Rev. Lett. **74**, 1633 (1995).
[6] G. Vignale and A. H. MacDonald, Phys. Rev. Lett. **76**, 2786 (1996).
[7] Yu. E. Lozovik and O. L. Berman, JETP **84**, 1027 (1997).
[8] A. Iyengar, J. Wang, H. A. Fertig, and L. Brey, Phys. Rev. B **75**, 125430 (2007).
[9] O. L. Berman, Yu. E. Lozovik, and G. Gumbs, Phys. Rev. B **77**, 155433 (2008).
[10] O. L. Berman, R. Ya. Kezerashvili, and Yu. E. Lozovik, Phys. Rev. B **78**, 035135 (2008).

[11] O. L. Berman, R. Ya. Kezerashvili, and Yu. E. Lozovik, Phys. Lett. A **372**, 6536 (2008).
[12] Yu. E. Lozovik and A. A. Sokolik, JETP Lett. **87**, 55 (2008).
[13] H. Min, R. Bistritzer, J.-J. Su, and A. H. MacDonald, Phys. Rev. B **78**, 121401(R) (2008).
[14] R. Bistritzer and A. H. MacDonald, Phys. Rev. Lett. **101**, 256406 (2008).
[15] M. Yu. Kharitonov and K. B. Efetov, Phys. Rev. B **78**, 241401(R) (2008).
[16] D. Haberer, D. V. Vyalikh, S. Taioli, B. Dora, M. Farjam, J. Fink, D. Marchenko, T. Pichler, K. Ziegler, S. Simonucci, M. S. Dresselhaus, M. Knupfer, B. Büchner, and A. Grüneis, Nano Lett. **10**, 3360 (2010).
[17] D. A. Abanin, A. V. Shytov, and L. S. Levitov, Phys. Rev. Lett. **105**, 086802 (2010).
[18] V. Lukose, R. Shankar, and G. Baskaran, Phys. Rev. Lett. **98**, 116802 (2007).
[19] J. Sabio, F. Sols, and F. Guinea, Phys. Rev. B **81**, 045428 (2010).
[20] A. A. Abrikosov, L. P. Gorkov, and I. E. Dzyaloshinski, *Methods of Quantum Field Theory in Statistical Physics* (Prentice-Hall, Englewood Cliffs, NJ, 1963).
[21] Yu. E. Lozovik and V. I. Yudson, Physica A **93**, 493 (1978).
[22] J. M. Kosterlitz and D. J. Thouless, J. Phys. C **6**, 1181 (1973); D. R. Nelson and J. M. Kosterlitz, Phys. Rev. Lett. **39**, 1201 (1977).
[23] V. Negoita, D. W. Snoke, and K. Eberl, Phys. Rev. B **60**, 2661 (1999).
[24] A. T. Hammack, L. V. Butov, L. Mouchliadis, A. L. Ivanov, and A. C. Gossard, Phys. Rev. B **76**, 193308 (2007).